Available online at www.sciencedirect.com
ScienceDirect
Biochemical and Biophysical Research Communications 353 (2007) 109–114
BBRC
www.elsevier.com/locate/ybbrc

Concerning the dynamic instability of actin homolog ParM

David Popp [a,*], Akihiro Yamamoto [b], Mitsusada Iwasa [a], Akihiro Narita [a], Kayo Maeda [a], Yuichiro Maéda [a,b,c]

[a] *ERATO "Actin Filament Dynamics" Project, Japan Science and Technology Corporation, c/o RIKEN Harima Institute at Spring 8, Kouto, Sayo, Hyogo 679-5148, Japan*
[b] *RIKEN Harima Institute at Spring 8, Laboratory for Structural Biochemistry, Kouto, Sayo, Hyogo 679-5148, Japan*
[c] *Nagoya University, Graduate School of Science, Division of Biological Science, Chikusa-ku, Nagoya 464-8602, Japan*

Received 18 November 2006
Available online 6 December 2006

Abstract

Using *in vitro* TIRF- and electron-microscopy, we reinvestigated the dynamics of native ParM, a prokaryotic DNA segregation protein and actin homolog. In contrast to a previous study, which used a cysteine ParM mutant, we find that the polymerization process of wild type ATP-ParM filaments consists of a polymerization phase and a subsequent steady state phase, which is dynamically unstable, like that of microtubules. We find that the apparent bidirectional polymerization of ParM, is not due to the intrinsic nature of this filament, but results from ParM forming randomly oriented bundles in the presence of crowding agents. Our results imply, that in the bacterium, ParM filaments spontaneously form bipolar bundles. Due to their intrinsic dynamic instability, ParM bundles can efficiently "search" the cytoplasmic lumen for DNA, bind it equally well at the bipolar ends and segregate it approximately symmetrically, by the insertion of ParM subunits at either end.

Keywords: ParM; Actin homolog; Bacterial segregation protein; TIRF microscopy; Dynamic instability; Molecular crowding; Bipolar bundles; Electron microscopy

Bacterial plasmids encode partitioning (*par*) loci that ensure ordered plasmid segregation prior to cell division. There are two types of *par* loci, those that encode actin-like ATPases and those that encode Walker-type ATPases. The *par* locus of the R1 drug-resistance plasmid encodes three components: a centromere-like site in the DNA (*parC*), a DNA binding protein (parR), and ParM, an actin-like protein bearing the ATPase activity [1]. These components form an assembly, that can be regarded as a primitive mitotic spindle, and it positions pairs of plasmids at opposite ends of the rod-shaped bacterium, ensuring equal distribution of the plasmids between the daughter cells. *In vivo*, ParM formed long filament bundles extending from pole to pole or from the middle of the cell to opposite poles [2]. These filaments are only visible in about 40% of the bacterial population at any given time, indicating that they are transient. R1 plasmids are located at the ends of the ParM filament, and it is thought that ParM polymerization is the driving force that pushes the plasmids to the opposite poles of a dividing bacterium [2].

Despite the low overall sequence identity between actin and ParM, the crystal structure of ParM is strikingly similar to that of actin. Moreover, ParM polymerizes into two-stranded helical filaments resembling those of conventional F-actin [3]. F-actin is a polar structure, which favors polymerization of the barbed end over the pointed end. At equilibrium, ATP–actin monomers associate with the barbed end and ADP–actin monomers dissociate from the pointed end, leading to treadmilling [4].

Recent fluorescence microscopy work on ParM, using ParM variants with a five residue extension at the C-terminus ending with a cysteine residue, in order to attach

* Corresponding author. Fax: +81 791 58 2836.
E-mail address: dpopp@spring8.or.jp (D. Popp).

0006-291X/$ - see front matter © 2006 Elsevier Inc. All rights reserved.
doi:10.1016/j.bbrc.2006.11.130

fluorescent probes covalently (ParM-Cys), yielded unexpected observations [5]. First, unlike F-actin, the ParM filament polymerized bidirectional, with equal polymerization rates at both ends. Second, after the initial rapid growth, the ParM filaments suddenly switched to rapid complete disassembly.

Here, we have reinvestigated the dynamics of ParM filament formation by use of the native ParM, without the five residue extension at the C-terminus, by TIRF- and electron-microscopy. We were motivated to do so, as it is known that modifications of actin at the C-terminus by either fluorescent dyes [6] or tags (Iwasa et al., unpublished) may influence the polymerization and steady state behavior as compared to the native protein. Given the close structural similarity between actin and ParM filaments [3], we thought, this could also be the case for ParM. Indeed, we find major differences compared to the previous investigation.

Our results indicate that wild type ParM has a strong tendency to form dynamically instable bidirectional bundles of several filaments in a crowded environment as found *in vivo* in the bacteria [2] and that this may be essential for the physiological function of ParM.

Materials and methods

Chemicals. Hepes was purchased from Dojindo. KCl, $MgCl_2$, DTT, hydrofluoric acid, potassium phosphate, KOH, and methyl cellulose 4000 (MC) were obtained from Wako. ATP, ATPγS and apyrase were from Sigma., Polyvinyl alcohol # 500 (PVA) was purchased from Kanto Chemical. Ficoll 70 was from Fluka. Alexa 488 carboxylic acid succinimidyl ester 6-isomer and 5-(and-6) carboxy tetramethylrhodamine succinimidyl ester were obtained from Invitrogen.

Proteins. Native ParM was overexpressed in *Escherichia coli* from pMD137 and purified as previously described [2]. The protein was either used fresh or was frozen in small quantities in Eppendorf tubes cooled to the temperature of liquid nitrogen. The protein concentration was determined using the Biorad or Ehresmann method [14]. Before experiments, the native ParM was dialyzed against ParM buffer (25 mM KCl, 1 mM $MgCl_2$, and 10 mM Hepes, pH 7.5) and lysines were labeled with Alexa 488 carboxylic acid succinimidyl ester 6-isomer or 5-(and-6) carboxy tetramethylrhodamine succinimidyl ester at a molar ratio of about 1 dye to 4 ParM over night at 4 °C similar as described for actin [15]. The reaction was quenched by adding 10 mM DTT. Protein was briefly centrifuged at high speed before use.

TIRF microscopy. Glass slides were cleaned by a short dip in concentrated hydrofluoric acid, followed by washes in 1 M KOH, and deionized and filtered water to remove all traces of acid and base and stored in ethanol until use. For our study of the time course of polymerization, ParM was diluted to an appropriate concentration, using ParM buffer in the presence of 10 mM DTT and various amounts of crowding agents (0.6–0.8% MC, 4–8% PVA, or 15–20% Ficoll 70). Depending on the experiment, ATP and ATPγS were added, mixed and applied either to a flow cell, which allowed exchange of solution, or ParM and nucleotide were directly mixed on the glass slide and covered with a glass slip.

ParM filaments labeled by fluorescent dye were observed with an inverted microscope (Nikon TE-2000), equipped with a Nikon-TIRF unit and an auto focus assist system (Nikon), which eliminated the usual problem of the objects drifting in the direction of depth. Samples were illuminated by either a green (Crystal Laser GCL-025 L) or a blue (Coherent Sapphire 488-20) laser, which were both mounted on a Nikon C1 laser unit. The illumination beam was collimated by a microscope objective lens (Nikon Plan Apo TIRF 60×, NA 1.45). Fluorescence images of ParM were recorded on a cooled CCD camera (Hamamatsu, ORCA II ER, C4742-98) and were stored on a custom-made PC, using the Hamamatsu Aquacosmos software. Filament length was analyzed using the programs Aquacosmos, ImageJ, and KaleidaGraph 3.6.

Electron microscopy. Samples, the same as used in TIRF microscopy, were applied to glow discharged, carbon-coated, copper grids, negatively stained with 1% uranyl acetate, blotted, air dried, and examined under a Jeol JEM-2010 HC microscope operated at 100 keV at a nominal magnification of 40,000.

Results and discussion

ParM polymerization dynamics and length distribution

Using TIRF microscopy, we examined the polymerization dynamics of recombinant wild type ParM filaments. The addition of ATP or ATPγS, a nonhydrolyzable ATP analog, started the elongation of the filament, which soon reached several micrometer in length (Fig. 1 and Supplementary material movies 1 and 2). Polymerization consisted of a rising phase followed by a steady state phase. The elongation phase was similar for both ATP- and ATPγS-

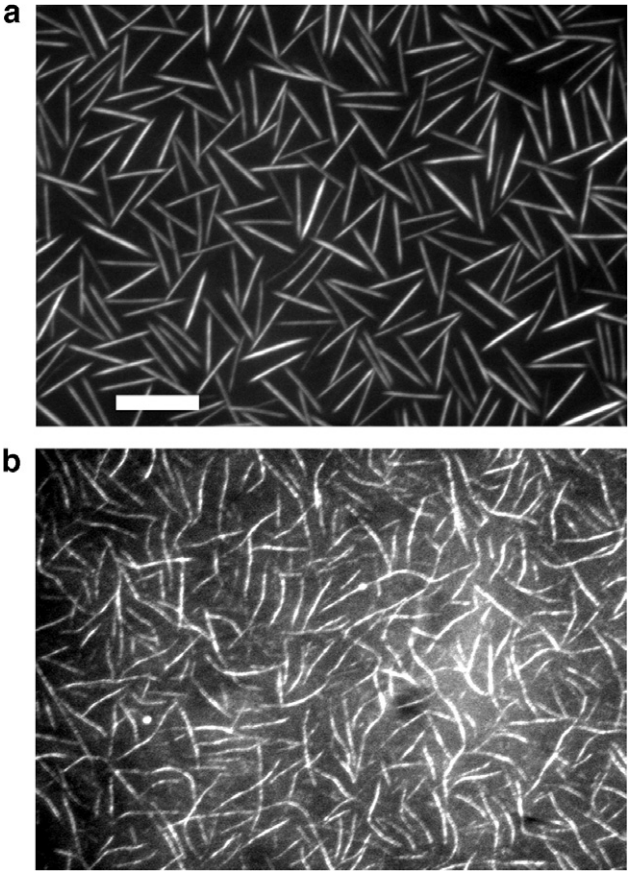

Fig. 1. Typical TIRF images of native ParM. The ParM concentration was 3.6 μM, with 8% PVA present. Images were taken 30 min after the initiation of polymerization, in the presence of 2 mM ATPγS (a), or in the presence of 10 mM ATP (b). Note the filaments are more irregular in the presence of ATP, due to the dynamic instability and the background is higher, due to a larger pool of free monomers (b). Scale bar, 10 μm (see Supplementary material for time-laps movies 1 and 2).

filaments (Fig. 2a and b), with an apparent polymerization rate constant of about 4 subunits/μM s. Yet the subsequent steady state phase differed. In the presence of ATPγS, the filament length fluctuations for all ParM concentrations studied were small, 5 subunits/s at most, which is likely due to the error in our length measurements. On the other hand, in the presence of ATP, the filaments underwent length changes with dramatically larger amplitudes, up to 100 subunits/s. The detailed steady state time courses (Fig. 2c) indicate that the ATP-ParM filaments abruptly switch from elongation to endwise disassembly and back again, similar to the behavior of microtubules [7]. It should be noted, that the switching in both directions seems to be stochastic in nature. In the presence of sufficient amounts of ATP, we never observed complete disassembly of the filaments. Filaments were observed even for several days, until the ATP was completely exhausted (see Supplementary material Fig. 1). Upon the depletion of ATP by the addition of apyrase, which converts ATP to ADP, the filaments disassembled completely (see Supplementary material movie 3). Our results differ from those previously obtained [5], where the ATP-ParM-Cys filaments rapidly polymerized, and then switched to complete disassembly within about 60 s.

Irrespective of the presence of ATP or ATPγS, wild type ParM filaments reached considerable lengths up to 10 μM (Fig. 1). This result differs from that in the previous study [5] in which the ATP-ParM-Cys filaments were maximally 1.5 μm long, independent of the ParM concentration, and only the ATPγS-ParM filaments grew to several micrometer in length. Shape and intensity of native ATP-ParM filaments appears more irregular compared to the rather straight and homogeneous ATPγS-filaments. This is due to the high dynamic instability of ATP-ParM filaments with subsequent larger mobility in the evanescent field (Fig. 1). The background in the presence of ATP is also significantly higher, as the instability of the filaments lead to a larger pool of free ParM monomers, compared with ATPγS, where at steady state basically all monomers are incorporated into stable filaments (Fig. 1).

Both the previous observations, that the ATP-ParM-Cys filaments only reached 1.5 μm in length, and that after

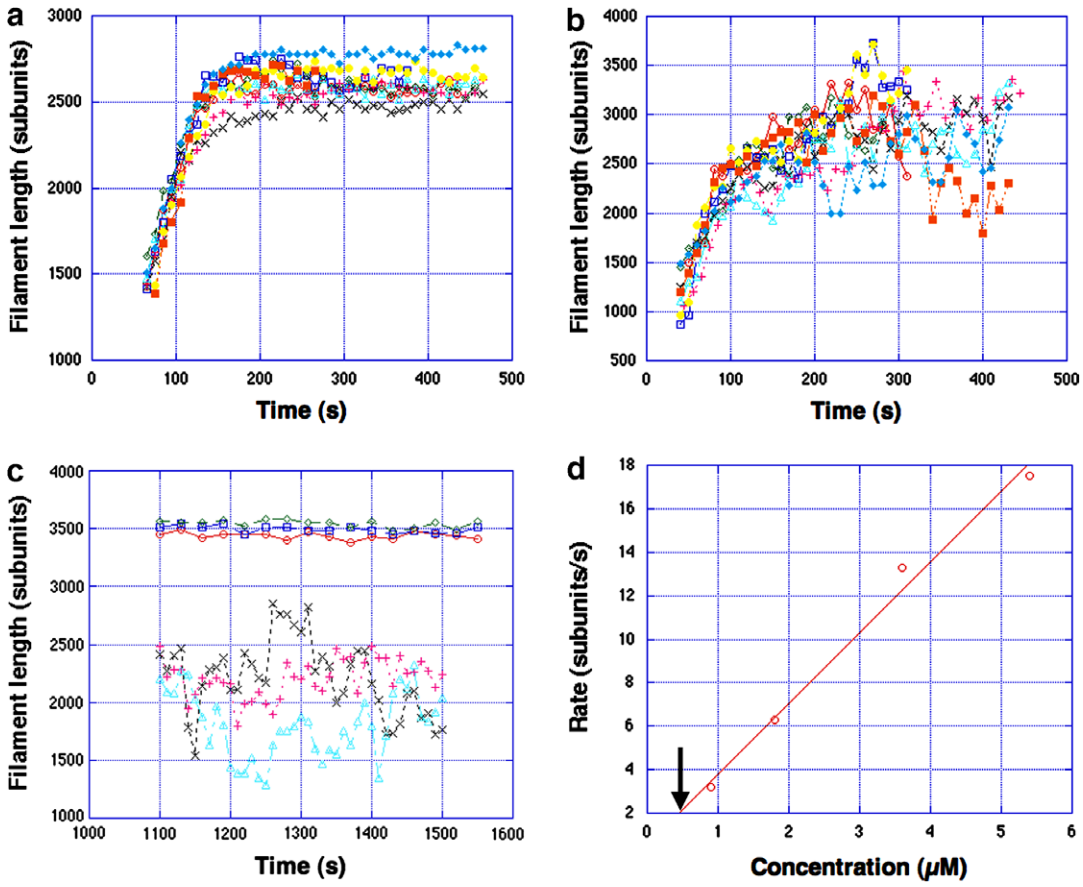

Fig. 2. Typical time courses of polymerization of native ParM filaments. The concentration of ParM was 3.6 μM as in Fig. 1. (a) In the presence of 2 mM ATPγS and 8% PVA. (b) In the presence of 10 mM ATP and 8% PVA. (c) A more detailed comparison of the dynamic instability of representative ATPγS-ParM (symbols in red, blue, green) and ATP-ParM filaments (symbols in black, light blue and pink) in the steady state. During the observations the filaments were frequently seen to assemble side-by-side (see Supplementary material movie 5). Once such an event occurred, we stopped the data analysis. On the ordinate, the filament length is expressed in terms of the number of subunits, where 380 subunits/μm is assumed. (d) The relationship between the average polymerization rates and the concentration of ParM filaments in the presence of ATPγS and 8% PVA. The arrow indicates the critical concentration for polymerization.

elongation the filaments abruptly started to disintegrate and proceed to total disassembly, indicates that the ATP-ParM filaments in the previous study was less stable than those used in the present study. We attribute the instability to the modification of the C-terminus of ParM in the previous work; the C-terminus was extended by adding five extra amino acids and a fluorescent probe was covalently attached to the extension. In contrast, in the present work, we used native ParM without the extension. In the case of actin, either the covalent attachment of fluorescent dyes at the C-terminus [6,13] or an extension of six histidine residues at the C-terminus (Iwasa et al., unpublished) substantially inhibit the polymerization. Given the close similarity between the F-actin and the ParM filament [3], this also seems likely for ParM.

The critical concentration

We determined the critical concentration of ATPγS-ParM filaments by plotting the relationship between the average polymerization rates and the ParM concentration (Fig. 3a). We find that polymerization velocity and protein concentration are linearly related. The intersection of the linear approximated slope with the abscissa generated a critical concentration of about 0.6 μM. The critical concentration for native ATP-ParM filaments is also in this range, as we could still see small, highly mobile filaments at 0.9 μM, moving in and out of the evanescent field (see Supplementary material movie 4). Thus the critical concentration of native ParM is at least a factor of three lower than that described previously for ParM-Cys [5].

Apparent bipolar elongation

We conducted dual color labeling experiments to reproduce the previous results on ParM-Cys mutant, which indicated that these filaments elongate at both ends with the same rate [5]. Native ParM labeled with rhodamine was polymerized into filaments in the flow cell by adding ATPγS. After the initial polymerization reached a steady state, ParM monomers labeled with Alexa 488 were introduced to the flow cell in the presence of ATPγS. Alexa-labeled ParM started to polymerize on the pre-existing rhodamine-labeled filaments. After equilibrium was reached, most of the filaments had red centers, with approximately equal amounts of green fluorescent pieces at each end (Fig. 4a), as previously reported. In the previous report, this observation was interpreted to indicate an intrinsic feature of individual ParM filaments, implying that the ParM filament is kinetically symmetric [5]. We believe, however, that the apparently symmetrical kinetics is due to the fact the ParM forms bidirectional bundles under the conditions generally employed in TIRF microscopy. All previous polymerization studies on actin [8–12]

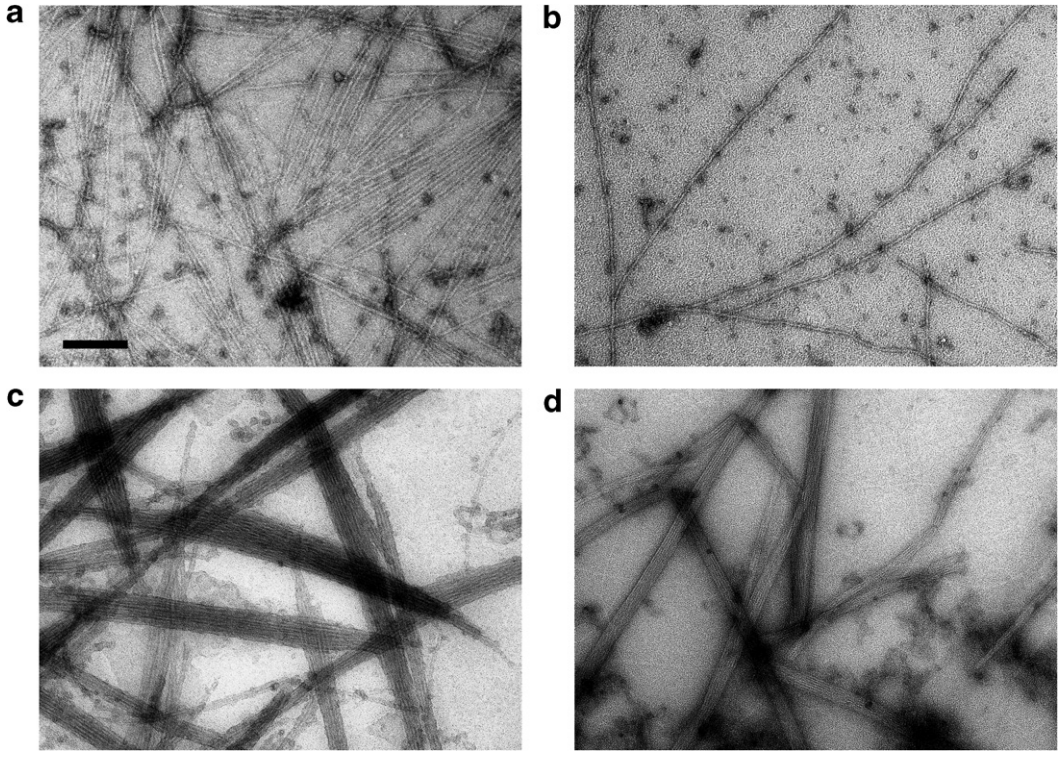

Fig. 3. Representative electron micrographs of ParM filaments. Conditions were the same as used for TIRF microscopy in Fig. 1. Protein solution was directly applied to glow discharged carbon-coated grids. (a) In the presence of 2 mM ATPγS, with no crowding agent present. (b) In the presence of 10 mM ATP and a small amount of a crowding agent, 0.15% MC 4000, which is insufficient for quantitative TIRF microscopy. (c) In the presence of 10 mM ATP and 0.8% MC. Note the marked shift to bundle formation. (d) In the presence of 10 mM ATP and 8% PVA. Scale bar, 200 nm. Note that bundle formation occurs at all protein concentrations studied (0.9–5.4 μM) in the presence 0.5–1% MC, 5–10% PVA, or 15–20% Ficoll 70.

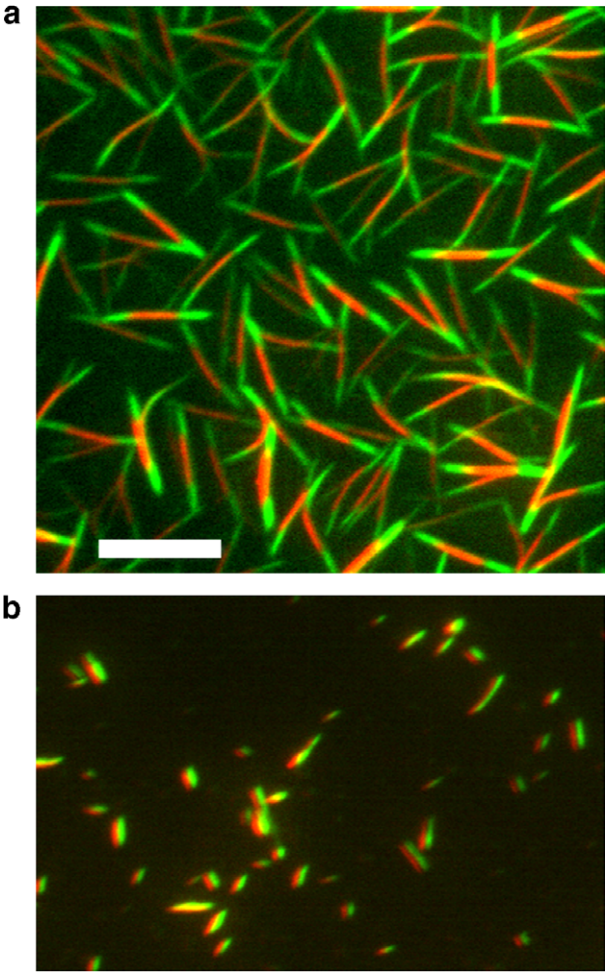

Fig. 4. (a) Direct observation of bipolar bundle elongation. Rhodamine labeled ParM (1 μM) was polymerized in the presence of 2 mM ATPγS and 20% Ficoll 70, on a hydrophilic glass surface for 30 min. Then, 1 μM Alexa 488 labeled monomeric ParM, in the presence of 2 mM ATPγS and 20% Ficoll 70, was introduced into the flow cell. After 30 min, dual images of rhodamine and Alexa labeled filaments were obtained. (b) A dual color annealing experiment indicates fragments of bundles assembled side-by-side, not annealed end-to-end. ParM filaments (2 μM), either labeled with rhodamine or Alexa, were polymerized separately in the presence of 8% PVA and 2 mM ATPγS overnight at 4 °C. Equal amounts of filaments were mixed and sheared 5 times through a 22 gauge needle using a syringe, placed onto the glass slide, and allowed to anneal. Note that the red and green images of some side-by-side assembled filaments appear to be shifted or slightly separated. This is because the images of the red and green filaments were taken a few seconds apart, as different lasers and filters have to be chosen in each case and during this time the filaments can move, as they are not firmly attached to the glass. This movement is also visible in (a), but it is smaller as in (b) because longer filaments are less mobile than shorter ones. Scale bar, 10 μm.

and ParM [5] that employed TIRF microscopy used crowding agents, like MC, PVA, or Ficoll 70, in order to prevent the vigorous Brownian movement of the filament, which hampers the attainment of a clear fluorescent image [10]. Yet it is known that crowding agents can bundle actin filaments under these conditions [12].

To clarify whether the apparent bipolar elongation observed, occurs with the isolated filament or with the filament bundle under crowding conditions, we studied the ParM filament by electron microscopy. In the presence of no or small amounts of crowding agents (0.15% MC or 1% PVA), conditions which are insufficient for quantitative TIRF microscopy, we observed almost entirely isolated ParM filaments in the presence of either ATP or ATPγS (Fig. 3) for all protein concentrations studied (0.9–5.4 μM). However, at the concentrations of crowding agents that are commonly used in TIRF observations of filamentous proteins (0.8% MC also used in the previous study [5], 6–8% PVA, or 15–20% Ficoll 70), the filament distribution at all ParM concentrations studied (0.9–5.4 μM), dramatically shifted from isolated filaments to bundles of several filaments (Fig. 3). Our EM studies indicate that the majority of the filaments, which were observed in the evanescent field, either in the previous work [5] or in the present study, must be filament bundles rather than individual filaments.

From our electron micrographs we do not know the polarities of the individual filaments within each bundle, as the shape of the ParM filaments do not show polarity at the present resolution. Nevertheless, we suppose that our bundles probably consist of randomly oriented filaments. This notion is supported, if not proved, by our dual color TIRF annealing experiment (Fig. 4b). Rhodamine-labeled ATPγS-ParM bundles and Alexa-labeled ATPγS-ParM bundles were mixed and fragmented by shearing, and the time course of reassembly was followed. If end-to-end annealing between fragmented bundles occurs, then the bundles would be alternately colored in the axial direction, as in Fig. 4a. Since no such pattern was observed, and since the two colors were parallel to each other, we concluded that the fragmented bundles assembled side-by-side. This indicates that each bundle probably consists of filaments of mixed polarities. With mixed polarities, the ends of each bundle cannot match each other, making end-to-end annealing of bundles unlikely. Side-by-side annealing is commonly observed during filament polymerization as well and our time-laps movies show this in real-time (see Supplementary material movie 5). Our results suggest that the apparent bipolar, symmetric elongation is due to the fact that the filaments form bipolar bundles. This interpretation makes sense, as previous EM analysis indicated that a single ParM filament is a polar, two-stranded, helix, which is very similar to F-actin [3] and it would be almost impossible to reconcile the single filaments polar structure with symmetric kinetic properties of elongation at either end.

Conclusion

In conclusion, our observations differ from the previous observations [5] in four points. First, whereas we have confirmed that the native ParM-ATP filaments exhibit dynamic instability in the steady state, this instability never brings about the sudden and complete disassembly of the native filaments. Second, in our observations, the native

ATP-ParM filament grows up to 10 μm long, whereas in the previous study, the filaments were only about 1.5 μm long. Third, the critical concentration of wild type ParM is at least 3-fold lower compared to the ParM-Cys mutant. Finally, the previous study attributed the apparent bipolar elongation to a property of the isolated filament, whereas our present study has interpreted that bipolar elongation occurs because the filaments form bundles with mixed polarities in response to crowding.

Based on the results presented here, we propose a mechanism for ParM filament segregation of plasmids in bacteria. First, due to the natural crowdedness inside bacteria, which is in the range of 30–40% of the total volume, and in the presence of ATP, ParM spontaneously polymerizes and the filaments form a bipolar bundle, as observed *in vivo* [2]. The bipolar bundle is advantageous for forming a complex with ParR-*parC*, since not only one but also several filaments contribute to capturing a pair of plasmids at either end of the bundle. In contrast, according to the previous study [5], a pair of plasmids is most likely captured by a single filament.

Second, in our proposal, the dynamic instability of the ATP-ParM filament results in prolonged states of depolymerization and polymerization, which interconvert frequently, just as in the microtubule [7]. Although the ParM filaments and microtubules are structurally quite different, it is interesting to note that both are designed to be unstable polymers, in order to search space most efficiently.

Acknowledgments

We thank Jakob Møller-Jensen, MRC, Cambridge, for his kind gift of the ParM plasmid and Harold P. Erickson, Duke University for suggestions on the manuscript.

Appendix A. Supplementary data

Supplementary data associated with this article can be found in the online version at doi:10.1016/j.bbrc.2006.11.130.

References

[1] G. Ebersbach, K. Gerdes, Plasmid segregation mechanisms, Annu. Rev. Genet. 39 (2005) 453–479.
[2] J. Moller-Jensen, J. Borch, M. Dam, R.B. Jensen, P. Roepstorff, K. Gerdes, Bacterial mitosis: ParM of plasmid R1 moves plasmid DNA by an actin-like insertional polymerization mechanism, Mol. Cell 12 (2003) 1477–1487.
[3] F. van den Ent, J. Moller-Jensen, L.A. Amos, K. Gerdes, J. Lowe, F-actin-like filaments formed by plasmid segregation protein ParM, EMBO J. 21 (2002) 6935–6943.
[4] N. Selve, A. Wegner, Rate of treadmilling of actin filaments in vitro, J. Mol. Biol. 187 (1986) 627–631.
[5] E.C. Garner, C.S. Campbell, R.D. Mullins, Dynamic instability in a DNA-segregating prokaryotic actin homolog, Science 306 (2004) 1021–1025.
[6] D.S. Kudryashov, M. Phillips, E. Reisler, Formation and destabilization of actin filaments with tetramethylrhodamine-modified actin, Biophys J. 87 (2004) 136–145.
[7] M.W. Kirschner, T. Mitchison, Microtubule dynamics, Nature 324 (1986) 621.
[8] J.R. Kuhn, T.D. Pollard, Real-time measurements of actin filament polymerization by total internal reflection fluorescence microscopy, Biophys J. 88 (2005) 1387–1402.
[9] I. Fujiwara, S. Takahashi, H. Tadakuma, T. Funatsu, S. Ishiwata, Microscopic analysis of polymerization dynamics with individual actin filaments, Nat. Cell. Biol. 4 (2002) 666–673.
[10] I. Fujiwara, S. Suetsugu, S. Uemura, T. Takenawa, S. Ishiwata, Visualization and force measurement of branching by Arp2/3 complex and N-WASP in actin filament, Biochem. Biophys. Res. Commun. 293 (2002) 1550–1555.
[11] K.J. Amann, T.D. Pollard, Direct real-time observation of actin filament branching mediated by Arp2/3 complex using total internal reflection fluorescence microscopy, Proc. Natl. Acad. Sci. USA 98 (2001) 15009–15013.
[12] D. Popp, A. Yamamoto, M. Iwasa, Y. Maeda, Direct visualization of actin nematic networks formation and dynamics, Biochem. Biophys. Res. Commun. 351 (2006) 348–353.
[13] L.R. Otterbein, P. Graceffa, R. Dominguez, The crystal structure of uncomplexed actin in the ADP state, Science 293 (2001) 708–711.
[14] B. Ehresmann, P. Imbault, J.H. Weil, Spectrophotometric determination of protein concentration in cell extracts containing tRNA's and rRNA's, Anal. Biochem. 54 (1973) 454–463.
[15] H. Isambert, P. Venier, A.C. Maggs, A. Fattoum, R. Kassab, D. Pantaloni, M.F. Carlier, Flexibility of actin filaments derived from thermal fluctuations. Effect of bound nucleotide, phalloidin, and muscle regulatory proteins, J. Biol. Chem. 270 (1995) 11437–11444.